REVISION 4

TITLE

ARMSTRONGITE FROM KHAN BOGDO (MONGOLIA): CRYSTAL STRUCTURE DETERMINATION BY SCXRD, EPMA AND INFRARED INVESTIGATION

Mesto Ernesto[1], Kaneva Ekaterina[1], Schingaro Emanuela[1], Vladykin Nikolay[2], Lacalamita Maria[1], Fernando Scordari[1]

[1]Dipartimento di Scienze della Terra e Geoambientali - Università degli Studi di Bari "Aldo Moro", via E. Orabona 4, I-70125 Bari, Italy.

[2]Institute of Geochemistry, Siberian Branch of the Russian Academy of Sciences, Irkutsk-33, Russia 664033

Submitted to: *American Mineralogist*

Word processor: *Word Microsoft Office 2003*

Address of the corresponding author:

Prof. Fernando Scordari

Dipartimento di Scienze della Terra e Geoambientali

Università degli Studi di Bari

Via Orabona 4, I-70125 Bari, Italy

e-mail: fernando.scordari@uniba.it

Phone 0039-080-5442587

Fax 0039-080-544259

ABSTRACT

The results of a combined electron probe microanalysis, single crystal X-ray diffraction and Fourier transform infrared study of a crystal of armstrongite from Khan Bogdo deposit (Gobi, Mongolia) are reported. Major element analysis provided (wt%): CaO 9.2(1), ZrO_2 20.9(2) and SiO_2 62.5(2). Significant concentrations of REE (0.45 wt%) were also detected. From single-crystal structural refinement, armstrongite resulted monoclinic (space group *C*2/*m*, *a* = 14.0178(7) Å, *b* = 14.1289(6) Å, *c* = 7.8366(3) Å, β = 109.436(3)°, *V* = 1463.6(1) Å^3, *Z* = 4) and twinned with two individuals rotated around a twin 2-fold axis parallel to [100]. The analyzed crystal was refined up to *R* = 3.3% (R_w = 2.9%). The structural refinement showed that the investigated armstrongite has only two water groups per formula unit consistent with the infrared analysis. Indeed, the occurrence in the infrared spectrum of the armstrongite (here reported for the first time) of two bending vibration bands at about 1640 and 1610 cm^{-1} testifies to the presence of two water groups environments. The results of this integrated approach converged to the following empirical formula (based on Si = 6 atoms per formula unit): $(Ca_{0.96}Ce_{0.01}Yb_{0.01})Zr_{0.99}Si_6O_{14.97} \bullet 2.02H_2O$. Finally, the studied mineral shows a framework density (FD = 21.86) lying in the range of zeolites and microporous heterosilicates with tetrahedral-octahedral frameworks. The determined crystal chemical features are relevant for the possible employment of this mineral or of its synthetic analogues for technological applications.

Keywords: armstrongite, microporous Zr-silicates, single crystal structure refinement, EPMA, infrared analysis, water groups

INTRODUCTION

Armstrongite, $CaZr[Si_6O_{15}] \cdot nH_2O$, ($2 \leq n \leq 3$), named after the American astronaut Neil A. Armstrong, is a rare mineral identified for the first time by Vladykin et al. (1973) in granite pegmatite and alkaline granites of the Khan Bogdo massif (Mongolia). From the same locality Vladykin (1983) and Vladykin and Kovalenko (2006) reported data from crystals of two generations of armstrongite. This mineral was also described in the canadian peralkaline granitic Strange Lake alkalic complex of the Québec-Labrador boundary (Jambor et al. 1987) in association with elpidite and gittinsite (Salvi and Williams-Jones 1995; Roelofsen and Veblen 1999).

Armstrongite belongs to the group of Zr-silicates having-general formula $[Zr_mSi_nO_{3m+2n}]^{-2m}$, and is characterized by a mixed framework of $[Si_6O_{15}]$ silicate sheets interlinked via ZrO_6 octahedra through vertex connection of octahedra and tetrahedra. According to Liebau's classification, armstrongite contains unbranched silicate single layers of $\{\boldsymbol{uB}, 1^2_\infty\}$ $[^3Si_6O_{15}]$ composition with only tertiary $[SiO_4]$ tetrahedra (Liebau 1985).

The stability of such polyhedral topology depends on the formation of almost equivalent Si-O-Si or Si-O-Zr bonds (Zubkova and Pushcharovsky 2008 and references therein).

Ghose et al. (1980) classified the armstrongite as a Zr-silicate belonging to the Zr-zeolite family together with catapleiite $(Na_2,Ca)Zr(Si_3O_9) \cdot 2H_2O$ (Ilyushin et al. 1981a), gaidonnayite $Na_2Zr(Si_3O_9) \cdot 2H_2O$ (Chao 1973), hilairite $Na_2Zr(Si_3O_9) \cdot 3H_2O$ (Ilyushin et al. 1981b), elpidite $Na_2Zr(Si_6O_{15}) \cdot 3H_2O$ (Cannillo et al. 1973), lemoynite $(Na_2Ca)Zr(Si_4O_{11}) \cdot 8H_2O$ (Le Page and Perault 1976). All these phases constitute alkali rocks and relative veins (Khomyakov 1995).

Structural details of armstrongite such as space group, content and location of water groups were still a matter of debate until this study. Possible space groups (*C*2, *Cm* and *C*2/*m*) were initially reported for Mongolian armstrongite polysynthetic twin with lattice parameters a = 14.04, b = 14.16, c = 7.81 Å and β = 109.55° (Vladykin et al. 1973). Kashaev and Sapozhnikov (1978) proposed the *C*2 space group for a twinned crystal from the same locality, basing on 319

reflections measured with photographic methods (De Jong-Bouman camera). However, their structure refinement converged to relatively high *R* value (13%) and gave negative temperature factors.

Jambor et al. (1987) studied *hk*0 → *hk*3, 0*kl* → 4*kl* and *h*0*l* → *h*4*l* level precession pictures of two blade crystals of the Canadian armstrongite which gave a monoclinic cell with systematic absences consistent with space groups *I*2/*m*, *I*2 or *Im*. The authors also obtained refined unit cell parameters (a = 13.599(9), b = 14.114(9), c = 7.833(4) Å and β = 103.41(5)°) from selected lines of Gandolfi camera powder film data. More recently, Kabalov et al. (2000) carrying out a Rietveld refinement on the Mongolian armstrongite, tested the space groups: *C*2, *Cm* and *C*2/*m*. Their best refinement (R = 2.14%) confirmed the space group (*C*2) and the structural model of Kashaev and Sapozhnikov (1978) and provided cell constants a = 14.018(1), b = 14.133(1), c = 7.840(1) Å and β = 109.40(1)°.

Regarding the content of water groups and their position in the structure, there is no agreement among researchers. Actually, 2.5 water groups per formula unit were initially found for the Mongolian armstrongite based on chemical analysis and density measurements (Vladykin et al. 1973). Kashaev and Sapozhnikov (1978) were unable to define the exact structural position of water groups due to the low quality of diffraction data whereas the subsequent structure model of Kabalov et al. (2000) provided three structurally different water group sites, out of which two lying on the 2-fold axis in the voids of zeolite like framework. Three water groups per formula unit were also obtained for the Canadian armstrongite using EPMA data and H_2O wt% calculated as difference from 100 wt% (Jambor et al. 1987).

In this work, a detailed crystal chemical investigation was carried out on a twinned crystal of armstrongite from Khan Bogdo massif (Gobi, Mongolia, Vladykin 1983; Vladykin and Kovalenko 2006) using a multi-analytical approach. In particular, a combination of electron probe microanalysis (EPMA), single crystal X-ray diffraction (SCXRD) and Fourier transform infrared spectroscopy (FTIR) was employed. It is noteworthy that for the first time an accurate

structure refinement from single crystal diffraction data and an infrared spectrum on armstrongite are here reported. It turned out that space group symmetry and content of water groups are different from those found in literature.

EXPERIMENTAL

Sample description and geological context

The Khan Bogdo alkali granite pluton is situated at the southern Gobi Desert, in the core of a Late Paleozoic Syncline, where island-arc calc-alkaline differentiated volcanics (of variable alkalinity) give way to the rift-related bimodal basalt–comendite–alkaline granite association. The Khan Bogdo pluton consists of typical alkaline granites (Vladykin et al. 1981; Vladykin 1983; Kovalenko et al. 2006) and constitutes an element of the extensive near-latitudinal South Gobi Belt of alkali granites, which is incorporated as the Gobi-Tien Shan Belt into the Late Paleozoic rift-related province of alkaline rocks of the Central Asian Foldbelt (Yarmolyuk and Kovalenko 1991). The sequence of rocks forming the pluton from older to younger intrusive phases (Vladykin 2013) is as follows: (1) coarse- to medium-grained elpidite-bearing alkaline granite of the main intrusive phase; (2) dikes of fine-grained ekerite, ekerite porphyry, layered alkaline granite consisting of alternating ekerites and pegmatites as well as pegmatoid alkaline granites and pegmatites; (3) fine- to medium-grained zircon-bearing alkaline granites (usually aegirine or arfvedsonite-aegirine and often miarolitic); (4) dikes of micrograined to glassy pantellerite; (5) dikes of porphyritic fine-grained alkali leucogranite; (6) dikes of microsyenite and micromonzonite; (7) rare carbonate and quartz–carbonate veins.

The areas enriched in transition elements and REE's ekerite dikes and pegmatites were characterized by Vladykin et al. (1981). The granites contain armstrongite, elpidite and unusual exsolved Nb-, Zr-, Ti-, and REE-silicates (Kovalenko et al. 2007). Vladykin (1983) and Vladykin and Kovalenko (2006), identified two generations of armstrongite into the Khan Bogdo massif. Armstrongite of the first generation forms columnar crystals along **b** axis which in

appearance resemble elpidite crystals. More often it occurs as aggregates of coarse grains and as the solid mass. Armstrongite of the second generation forms the tangled-fibrous aggregates which cement the large grains of armstrongite of the first generation. The crystal investigated here has been selected from the same rock sample (608/19a) in Vladykin (1983) and Vladykin and Kovalenko (2006). The picture of the host rock with the two generations of armstrongite is shown in Figure 1. The second generation armstrongite occurs in interstices and voids between microcline and grains of the first generation armstrongite.

Chemical analysis

Electron probe microanalysis was carried out on a single crystal of the studied second generation armstrongite embedded in epoxy resin, polished and then carbon coated. The same crystal was used for X-ray analysis. Henceforth the sample is referred to as Arm_KB_2.

A JEOL JXA-8200 electron microprobe operating at 15 kV accelerating voltage, 5 nA sample current, ~ 1 μm spot size and 40 s counting time was used. Full wavelength dispersive spectrometry (WDS) mode was employed. The used standards for major, minor and REE components were: wollastonite (Si), anorthite (Al, Ca), omphacite (Na), olivine (Mg), K-feldspar (K), Zr-jarosite (Zr), ilmenite (Ti), Cr pure (Cr), rhodonite (Mn, Zn), fayalite (Fe), celestine (Sr) sanbornite (Ba), La-phosphate (La), Ce-phosphate (Ce), Pr-phosphate (Pr), Nd-phosphate (Nd), Sm-phosphate (Sm), Eu-phosphate (Eu), Gd-phosphate (Gd), Dy-phosphate (Dy), Ho-phosphate (Ho), Er-phosphate (Er), Yb-phosphate (Yb), Lu-phosphate (Lu).

A Phi-Rho-Z routine was employed for the conversion from X-ray counts to oxide weight percentages (wt. %). The average composition (determined over four spots) is reported in Table 1 and compared to those of other armstrongite compositions found in the literature.

Structural analysis

Crystal-structural determination was performed with a Bruker AXS X8 APEXII automated diffractometer equipped with a four-circle Kappa goniometer, a CCD detector, and a monochromatized MoKα radiation. Operating conditions were: 50 kV and 30 mA, crystal-to-detector distance of 40 mm. The collection strategy was optimized with the COSMO program in the APEX2 suite package (Bruker 2003a) and the entire Ewald sphere (±h, ±k, ±l) up to $\theta_{max} \sim$ 40° was recorded by a combination of several ω and ϕ rotation sets, with 0.5° scan width and 10-20 s per frame exposure time. The SAINT package was used for the extraction of the reflection intensities and for the correction of the Lorentz-polarization (Bruker 2003b) effect. The Arm_KB_2 crystal was found to be monoclinic and twinned. CELL_NOW program (Sheldrick 2003a) identified two individuals rotated around a 2-fold twin axis parallel to [100]. The TWINABS software provided for a semi-empirical absorption correction (Sheldrick 2003b). The XPREP software was used for determination of the space group and in the calculation of the intensity statistics. The suggested space group was *C*2/*m*. The structure was solved using the charge flipping algorithm (Palatinus and Chapuis 2007), and the space group *C*2/*m* was confirmed by the analysis of the reconstructed electronic density.

The structure refinement was then performed against F_o in the space group *C*2/*m* using the program CRYSTALS (Betteridge et al. 2003). Reflections with $I > 3\sigma(I)$ were considered as observed and the refined parameters were: overall and twin domain scale factors, atomic positions, and anisotropic atomic displacement parameters. Ionized scattering factors were used for octahedral and Ca-polyhedral sites whereas neutral scattering factors were employed for anion and tetrahedral sites.

The final fully anisotropic refinement converged to $R = 3.3$ % ($R_w = 2.9$ %) and yielded the following proportion of the twin individuals 0.6176(4): 0.3824(4) (Table 2).

The difference Fourier map showed the two highest peaks of about 2.5 $e^-/Å^3$ and 1.6 $e^-/Å^3$ at (0.02, 0.00, 0.10) and (0, 0, 0), respectively. The first one was distant about 1.7 Å from the O6

oxygen, whereas the second one had no near contacts. Any attempt to model the two residual peaks as oxygen atoms led to physically unacceptable results (i.e. very large atomic displacement parameters, $U_{iso} \sim 3.5$ Å^2). Eventually, they have been considered residuals in the Fourier difference map with no chemical meaning. The H atoms were all located geometrically, and were initially refined with soft restraints on the bond lengths (i.e., O-H = 0.90(2) Å, see also Plàsil et al. 2011) and angles (H-O-H = 104(2)°) to regularize their geometry and with U_{iso}(H) from 1.2 to 1.5 U_{eq} with respect to that of the parent oxygen. Subsequently, their positions were refined with riding constraints (Cooper et al. 2010).

Summary data about the single crystal, the data-collection parameters and the structure refinement are listed in Table 2, whereas final atomic coordinates, site occupancies, equivalent isotropic and anisotropic displacement parameters are reported in Table 3. Relevant cation-anion bond lengths, polyhedra volumes and mean atomic numbers are given in Table 4.

Infrared analysis

The attempt to perform a micro-FTIR (Fourier Transform Infrared) analysis on the Arm_KB_2 crystal resulted in a very scattered spectrum due to the small crystal size and to the surface roughness. Therefore, FTIR measurement was carried out using a KBr pellet with an armstrongite-to-KBr weight ratio of 1:50. The pellet was then dried for 4h at 120°C to eliminate the absorbed water. A Nicolet Avatar FTIR spectrometer equipped with a deuterated tryglicine sulphate (DTGS) detector and a KBr beamsplitter was used. Spectrum was acquired from 4000 to 400 cm^{-1} by adding 128 scans with a nominal resolution of 4 cm^{-1} and a mirror velocity of 0.6329 cm/s.

RESULTS AND DISCUSSION

Chemical composition

The results of the EPMA investigation on the Arm_KB_2 crystal are compared, in Table 1, with the chemical composition of all the armstrongite so far studied. Apart from CaO, ZrO_2 and SiO_2, the amounts of Na_2O, Al_2O_3, K_2O, TiO_2 and MnO resulted very low or close the instrumental detection limit in the studied crystal. Significant concentrations of Ce_2O_3, Eu_2O_3, and Yb_2O_3 were measured, yielding a total of rare earth element (REE) content of 0.45 wt% . This value is much lower than that (1.30 wt%) calculated from data in Vladykin and Kovalenko (2006) for other crystals from the same rock sample. In addition, Arm_KB_2 crystal shows a higher SiO_2, ZrO_2 and CaO, and a remarkably lower Na_2O content with respect to the armstrongite composition in Vladykin (1983) and in Vladykin and Kovalenko (2006), see Table 1. In particular, the chemical composition of the studied crystal seems to approximate that of the first armstrongite generation, according to Vladykin et al. (1973). Finally, we observe that substantial similarities exist between the studied and the Canadian armstrongite composition in Jambor et al. (1987) and Salvi and Williams-Jones (1995), see Table 1.

Structure description and crystal chemistry

As reported in the **Introduction** section, the assignment of the armstrongite space group has been somewhat debated. Our refinement result on the Arm_KB_2 crystal, for the first time from single crystal data, shows unequivocally that the investigated sample crystallizes in space group *C*2/*m*. The obtained structural model is generally consistent with that proposed by Kabalov et al. (2000) but provides much better defined geometrical details and crystal chemical parameters (see Tables 4, 5).

To describe the armstrongite structure we start with the wollastonite-type chain (Figure 2a). The condensation of two of these chains results in a xonotlite-like chain (Haile and Wuensch 1997) (Figure 2b). Similar chains have been found also in vlasovite and miserite (Sokolova at al. 2006; Kaneva et al. 2013). The condensation of the xonotlite-like-chains, running along **b** axis, results into the arrangement of the tetrahedra in sheets showing four- and six-member rings

alternating along [010] and four- and eight-member rings alternating along [100] (Figure 2c). These sheets have $[Si_6O_{15}]^{6-}$ composition. Projections down to [010] and [100] axes of this radical are shown in Figure 2d and 2e, respectively. Silicate $[Si_6O_{15}]$ sheets are connected by vertices to ZrO_6 octahedra to give the $(ZrSi_6O_{15})^{2-}$ heterogeneous framework. The seven-fold coordination, $CaO_5(H_2O)_2$, polyhedra are connected by edges to ZrO_6 octahedra, to form columns running parallel to [010] (Figure 2f). Figure 2b shows two possible ideal distances between tetrahedra, whereas in Figures 2c to 2e those of the studied sample are reported. Such distances are comparable with the pore size of microporous silicates (Ferraris and Merlino 2005).

Table 2 shows that refined cell constants of the studied armstrongite are very close to those reported for other specimen in the literature (Vladykin et al. 1973; Kabalov et al. 2000). This is also true for those found by Jambor et al. 1987 (a = 14.031, b = 14.114, c = 7.833 Å, β = 109.48° when reported in the same setting as used here). Table 4, instead, evidences that, differently from Kabalov et al. (2000), the values of mean bond distances and volumes of the three independent Si1, Si2 and Si3 polyhedra are similar to each other (~ 1.61 Å and 2.13 $Å^3$, respectively). In addition, Kabalov et al. (2000) recorded a notable elongation of shared Si-O bond lengths ($<Si\text{-}O_{sh}>$ ~ 1.63 Å) with respect to unshared ones ($<Si\text{-}O_{ush}>$ ~ 1.58 Å), but this feature is less pronounced in the studied armstrongite ($<Si\text{-}O_{sh}>$ ~ 1.62 Å, $<Si\text{-}O_{ush}>$ ~ 1.59 Å), see Table 4. The distance (2.045(1) Å) between the Zr cation and the O9 oxygen which is involved in the linkage between octahedra and silicate sheets is shorter than the average of the remaining ones (~ 2.11 Å, Table 4).

In order to bring the O atoms sufficiently close to Zr cations, corrugation of the silicate layers are required. Such corrugation was evaluated as departure from coplanarity of the unshared O atoms along [100] and [010] (see Table 5). The studied armstrongite indicates that corrugation is anisotropic, i.e. it is greater along the [010] than in the [100] directions. The calculation was also performed on data from Kabalov et al. (2000) evidencing similar, even if

less accurate for the method they use, relative variations in that sample and in the crystal of the present study.

In the seven-fold Ca polyhedron, the distances of the Ca cation from the O10 and O11 oxygens are shorter than the remaining ones (Table 4). The latter oxygens are involved in the formation of two water groups in our armstrongite. This result is different from that of Kabalov et al. (2000) who recognized, besides the two water groups found in our structure, a third molecule split on two sites (O_W19, O_W20) lying on the 2-fold axis. Our findings are also supported by the void analysis carried out by means of Platon program (Spek 2009), which indicates that the unit cell contains no residual solvent accessible cavities. In addition, evidence of only two structurally different water groups in the studied sample was also derived by infrared analysis (see below).

Considering the above results, the following crystal chemical formula can be proposed for the studied armstrongite: $(Ca_{0.96}Ce_{0.01}Yb_{0.01})Zr_{0.99}Si_6O_{14.97} \bullet 2.02H_2O$. This formula was calculated on the basis of Si = 6 atoms per formula unit (apfu). A satisfactory agreement between mean electron numbers and average interatomic distances as derived by X-ray and EPMA measurements was found (Table 4). The interatomic distances have been calculated using the Shannon ionic radii (Shannon 1976). The formula of the armstrongite calculated on the basis of 6 Si apfu from the data in Vladykin (1983) and in Vladykin and Kovalenko (2006) gives: $(Ca_{0.82}Na_{0.08}\ Fe^{3+}_{0.08}Ce_{0.01})Zr_{0.95}Si_6O_{14.90} \bullet 3.03H_2O$. In this case, the lower concentration of Ca atoms with respect to that of the studied sample, is balanced mainly by Na and Fe^{3+} atoms.

Hydrogen speciation

Figure 3 illustrates the infrared spectrum obtained on a powder pellet of the studied armstrongite in the range 4000 to 400 cm^{-1}. It is similar but better resolved with respect to that collected for the single crystal used in the structure refinement (not shown). To the best of our

290 knowledge, no infrared characterization of the armstrongite has been documented in the
291 literature.

292 The hydrogen absorption bands occur in the region extending from 4000 to 1500 cm^{-1}
293 whereas the silicon and zircon framework vibration bands are observed in the region from 1500
294 to 400 cm^{-1}. Focusing on the hydrogen region, the broad absorption extending from 3700 to 2800
295 cm^{-1} is due to water groups stretching vibrations having characteristic bending vibration modes
296 at ~ 1640 and 1610 cm^{-1}. The latter bands are indicative of two water groups environments and
297 are consistent with the results of the structure refinement (Table 3). The occurrence of two water
298 groups environments has been already proposed for other zeolite-like zircon-silicates
299 (Grigor'eva et al. 2011; Zubkova et al. 2011; Yakubovich et al. 2013). More generally, infrared
300 spectra features found in this study are in agreement with previous reports for minerals with
301 similar compositions (see list in Table 6).

302 The correct assignment of the 1640 and 1610 cm^{-1} bands to the bending vibration of the
303 H101-O_w10-H101' and H111-O_w11-H111' molecules is not straightforward. It is known that the
304 frequencies of the water groups bending modes in a crystal depend on three parameters: 1) the
305 strength of hydrogen bonds between H atoms of water groups and the local environment; 2) the
306 interaction between the oxygen atom and the nearest cation; 3) the geometry of water groups, i.e.
307 the value of the H-O-H angle (Kolesov 2006).

308 The strength of the hydrogen bonds may be estimated starting from the valence at the
309 O_w10 and O_w11 atoms. According to Ferraris and Ivaldi (1988), the most reliable bond valence
310 (s) calculation is that based on the O·····O distances using the relationship: $s = (R/R_0)^{-b} + k$ where
311 R is the refined bond length whereas R_0, b and k are empirical constants. The values calculated
312 for the O_w10 and O_w11 oxygens were very close (i.e. from 0.07 to 0.12 and from 0.09 to 0.13
313 v.u., respectively) yielding no noticeable effects on the observed water groups bending
314 frequencies.

315 The structural formula [i.e., $(Ca_{0.96}Ce_{0.01}Yb_{0.01})Zr_{0.99}Si_6O_{14.97} \bullet 2.02H_2O$] indicates that
316 there are no significant cation substitutions affecting the Ca-polyhedron as well as the
317 neighbouring ZrO_6 octahedra and SiO_4 tetrahedra. Accordingly, the O_w10 and O_w11 sites have
318 the same local chemical environments. The slight differences in Ca-O_w10, Ca-O_w11 bond
319 distances (see Table 4), result in close values of bond valence calculations (s = 0.40 vs 0.37
320 respectively, following the relationship in Brown and Altermatt 1985). On the basis of the
321 experimental and theoretical considerations, the bending frequencies of water groups should
322 increase with a decrease in the strength of this interaction (Falk 1984; Falk et al. 1986).
323 Therefore, the observed 1640 and 1610 cm^{-1} bands in the spectrum of the studied armstrongite
324 could be assigned to the bending vibrations of the H111-O_w11-H111' and H101-O_w10-H101'
325 molecules, respectively.
326 Finally, the effect of the geometry of the two water groups on the bending modes
327 frequencies of the studied armstrongite could not be assessed because the definition of the H-O-
328 H angle itself requires the correct localization of the hydrogen atom by means of neutron
329 diffraction measurements at low temperature (Kolesov 2006).
330
331 **Comparison between armstrongite and elpidite**
332 The studied armstrongite was found in the Khan Bogdo alkaline granites massif in
333 association with elpidite which has the chemical formula $(Na,Ca,\square)_2Zr[Si_6O_{15}] \bullet 2.8H_2O$
334 (Sapozhnikov and Kashaev 1978). The Armstrongite and elpidite $[Na_2Zr(Si_6O_{15}) \bullet 3H_2O]$
335 heteropolyhedral framework show some topological similarities. Indeed, both minerals are
336 characterized by heteropolyhedral chains with $[Zr_2Si_4O_{12}]$ composition, but these chains are
337 connected by mirror planes in elpidite, and by rotation around a two-fold axis in armstrongite
338 (Figure 4); furthermore, elpidite has a second Na site in the plane containing the octahedra. In
339 elpidite, Na-polyhedra and ZrO_6 octahedra form a column running parallel to [100] (Figure 4a),
340 whereas in armstrongite Ca-polyhedra and ZrO_6 octahedra are parallel to [010] (Figure 4b).

The two mineral structures can be geometrically obtained from a similar single subcell (Figure 5). In elpidite it is approximately a cube having edges of about 7.2 Å, lying in the region: $x = 0$ - 1, $y = 0 – ½$, $z = ¼$ - ¾ while for the investigated armstronigite, the subcell lies in the axes range: $x = 0 – ½$, $y = 0 – ½$ and $z = ½$ - 3/2. The unit cell of elpidite can be obtained by translation of this subcell of $b/2$ along the [010] and then reflecting the obtained volume with respect to a mirror plane parallel to (001) and through the tetrahedron corners adjoining to the ZrO_6 octahedra. Shifting this subcell once along the x axis and reflecting its volume with respect to the mirror plane normal to the **b** axis, the unit cell of armstrongite is obtained. Conversely, the reconstruction of the armstrongite unit cell in $C2$ space group was described by Sapozhnikov and Kashaev (1978) by means of a subcell translation along x followed by a translation of its volume along y.

However, the exact fit of the elpidite and armstrongite crystal structures may be obtained by means of small polyhedral rotations and distortions (Roelofsen and Veblen 1999). The same authors proposed the $Na_2Zr[Si_6O_{15}] \cdot 3H_2O + Ca^{2+} \rightarrow CaZr[Si_6O_{15}] \cdot 3H_2O + 2Na^{+}$ reaction to represent the replacement of the magmatic elpidite by armstrongite in the subsolvus granite of the Strange Lake peralkaline complex (Canada). Finally, Kabalov et al. (2000) hypothesized the origin of the twinning in armstrongite as a consequence of the formation of elpidite-like modules at the border of the twin domains and described these minerals in terms of a polysomatic-series.

IMPLICATIONS

In the last years great attention has been devoted to the properties of microporous minerals whose structure is based on a mixed tetrahedral-octahedral framework. In the case of armstrongite, the mixed framework of silicate sheets and ZrO_6 octahedra forms cavities occupied by Ca-exchangeable cations having seven-fold coordination.

In the present work, the accurate atomic positions, as derived from structure refinement of high quality diffraction data, allowed the reliable determination of the cavities size in the

studied structure. On the other hand, the framework density, defined as the number of framework knots per 1000 $Å^3$ (FD, from Chukanov and Pekov 2005), has been proposed as the parameter defining the capability of ion exchange of microporous minerals. For this armstrongite specimen, the calculated framework density is 21.86, a value lying in the range (from 14 to 22) found for zeolites and microporous heterosilicates with framework of tetrahedra and octahedra. As a consequence, the detailed crystal chemical features of the studied mineral can help to determine their potential, as materials alternative to zeolites, for their possible usage in different fields, from environmental protection to industrial applications.

ACKNOWLEDGMENTS

We thank Prof. Stefano Poli for the facilities at the Electron Microprobe Laboratory of the Dipartimento di Scienze della Terra, Università di Milano. Thanks are due to the Associate Editor, Martin Kunz, and the Referees Natalia Zubkova and Joel Grice that contributed to improve the manuscript. This work was supported by the grants from the Italian Ministry of University and Research (PRIN 2010-2011) and from Fondazione Cassa di Risparmio di Puglia.

REFERENCES

Betteridge, P.W., Carruthers, J.R., Cooper, R.I., Prout, K., and Watkin, D.J. (2003) Crystals version 12: software for guided crystal structure analysis. Journal of Applied Crystallography, 36, 1487.

Brown, I.D. and Altermatt, D. (1985) Bond-valence parameters obtained from a systematic analysis of the inorganic crystal structure database. Acta Crystallographica, B41, 244-247.

Bruker (2003a) APEX2. Bruker AXS Inc., Madison, Wisconsin, USA

Bruker (2003b) SAINT. Bruker AXS Inc., Madison, Wisconsin, USA

392 Cannillo, E., Rossi, G., and Ungaretti, L. (1973) The crystal structure of elpidite. American
393 Mineralogist, 58, 106-109.
394 Chao, G.Y. (1973) The crystal structure of gaidonnayite, orthorhombic $Na_2ZrSi_3O_9 \cdot 2H_2O$.
395 Canadian Mineralogist, 12, 143-149.
396 Chao, G.Y. (1978) Monteregianite, a new hydrous sodium potassium yttrium silicate mineral
397 from Mont St-Hilaire, Québec. Canadian Mineralogist, 16, 561-565.
398 Chukanov, N.V. and Pekov, I.V. (2005) Heterosilicates with tetrahedral-octahedral frameworks:
399 mineralogical and crystal-chemical aspects. In: G. Ferraris and S. Merlino, Eds., Micro- and
400 mesoporous mineral phases, 57, 105-143. Reviews in Mineralogy & Geochemistry,
401 Mineralogical Society of America, Chantilly, Virginia.
402 Cooper, R.I., Thompson, A. L., and Watkin, D.J. (2010) *CRYSTALS* enhancements: dealing with
403 hydrogen atoms in refinement. Journal of Applied Crystallography, 43, 1100-1107.
404 Falk, M. (1984) The frequency of the H-O-H bending fundamental in solids and liquids.
405 Spectrochimica Acta, 40A, 43-48.
406 Falk, M., Flakus, H.T., and Boyd, R.J. (1986) Ab initio CSF calculation of the effect of water
407 anion and water cations on the vibrational frequencies of water. Spectrochimica Acta, 42A,
408 175-180.
409 Ferraris, G. and Ivaldi, G. (1988) Bond valence *vs* bond length in O···O hydrogen bonds. Acta
410 Crystallographica, B44, 341-344.
411 Ferraris, G. and Merlino, S. (2005) Micro- and mesoporous mineral phases, 57, 1-448. Reviews
412 in Mineralogy & Geochemistry, Mineralogical Society of America, Chantilly, Virginia.
413 Ghose, S., Che'ng, W., and Chao, G.Y. (1980) Petarasite, $Na_5Zr_2Si_6O_{18}$ (Cl, OH)•$2H_2O$, a
414 zeolite-type zirconosilicate. Canadian Mineralogist, 18, 503-509.
415 Grigor'eva, A.A., Zubkova, N.V., Pekov, I.V., Kolitsch, U., Pushcharovsky, D.Yu., Vigasina,
416 M.F., Giester, G., Dordevic, T., Tillmanns, E., and Chukanov, N.V. (2011) Crystal chemistry

417 of elpidite from Khan Bogdo (Mongolia) and its K- and Rb-exchanged forms.
418 Crystallography Reports, 56(5), 832-841.
419 Haile, S.M. and Wuensch, B.J. (1997) Comparison of the crystal chemistry od selected MSi_6O_{15}-
420 based silicates. American Mineralogist, 82, 1141-1149.
421 Ilyushin, G.D., Voronkov, A.A., Ilyukhin, V.V., Nevskii, N.N., and Belov, N.V. (1981a) Crystal
422 structure of natural monoclinic catapleiite $Na_2ZrSi_3O_9 \bullet 2H_2O$. Doklady Akademii Nauk SSSR
423 260, 623-627. (in Russian)
424 Ilyushin, G.D., Voronkov, A.A., Nevskii, N.N., Ilyukhin, V.V., and Belov, N.V. (1981b) Crystal
425 structure of hilairite, $Na_2ZrSi_3O_9 \bullet 3H_2O$. Doklady Akademii Nauk SSSR, 260, 1118-1120. (in
426 Russian)
427 Jambor, J.L., Roberts, A.L., and Grice, J.D. (1987) Armstrongite from the Strange Lake Alkalic
428 Complex, on the Quebec-Labrador Boundary, Canada. Powder Diffraction, 2, 2-4.
429 Johnsen, O. and Grice, J.D. (1999) The crystal chemistry of the eudialyte group. Canadian
430 Mineralogist, 37, 865-891.
431 Kabalov, Yu.K., Zubkova, N.V., Pushcharovsky, D.Yu., Schneider, J., and Sapozhnikov, A.N.
432 (2000) Powder Rietveld refinement of armstrongite, $CaZr[Si_6O_{15}] \cdot 3H_2O$. Zeitschrift für
433 Kristallographie, 215, 757-761.
434 Kaneva, E., Lacalamita, M., Mesto, E., Schingaro, E., Scordari, F., and Vladykin N.V. (2013)
435 Structure and modeling of disorder in miserite from the Murun (Russia) and Dara-i-Pioz
436 (Tajikistan) massifs. Physics and Chemistry of Minerals, 41, 49-63.
437 Kashaev, A.A. and Sapozhnikov, A.N. (1978) Crystal structure of armstrongite. Kristallografiya
438 (Soviet Physics - Crystallography), 23, 956-961.
439 Khomyakov, A.P. (1995) Mineralogy of hyperagrpaitic alkaline rocks. Oxford: Clarendon Press.
440 Kolesov, B.A. (2006) Raman spectra of single H_2O molecules isolated in cavities of crystals.
441 Journal of structural chemistry, 47, 21-34.

442 Kovalenko, V.I., Yarmoluyk, V.V., Sal'nikova, E.B., Kozlovsky, A.M., Kotov, A.B., Kovach,
443 V.P., Savatenkov, V.M., Vladykin, N.V., and Ponomarchuk, V.A. (2006) Geology,
444 Geochronology, and Geodynamics of the Khan Bogd alkali granite pluton in southern
445 Mongolia. Geotectonics, 40(6), 450-466.
446 Kovalenko, V.I., Yarmolyuk, V.V., Kozlovsky, A.M., Kovach, V.P., Sal'nikova, E.B., Kotov,
447 A.B., and Vladykin, N.V. (2007) Two types of magma sources of rare-metal alkali granites.
448 Geology of Ore Deposits, 49 (6), 442-466.
449 Le Page, Y. and Perrault, G. (1976) Structure cristalline de la lemoynite
450 $(Na, K)_2CaZr_2Si_{10}O_{26}$, 5-6 H_2O. Canadian Mineralogist, 14, 132-138.
451 Liebau, F. (1985) Structural chemistry of silicates. Structure, bonding, and classification, 347 p.
452 Springer-Verlag, Berlin Heidelberg New York Tokyo.
453 Palatinus, L. and Chapuis, G. (2007) *SUPERFLIP*- a computer program for the solution of
454 crystal structures by charge flipping in arbitrary dimensions. Journal of Applied
455 Crystallography, 40, 786-790.
456 Perrault, G., Semenov, E.I., Bikova, A.V., and Capitonova, T.A. (1969) La lemoynite, un
457 nouveau silicate hydraté de zirconium et de sodium de St. Hilaire, Québec. Canadian
458 Mineralogist, 9, 585-596.
459 Plášil, J., Fejfarová, K., Novák, M., Dušek, M., Škoda, R., Hloušek, J., Čejka, J., Majzlan, J.,
460 Sejkora, J., Machovič, V., and Talla, D. (2011) Běhounekite, $U(SO_4)_2(H_2O)_4$, from Jàchymov
461 (St Joachimsthal), Czech Republic: the first natural U^{4+} sulphate. Mineralogical Magazine,
462 75(6), 2739-2753.
463 Renner, B. and Lehmann, G. (1986) Correlation of angular and bond length distortions in TO_4
464 units in crystals. Zeitschrift für Kristallographie, 175, 43–59.
465 Robinson, K., Gibbs, G.V., and Ribbe, P.H. (1971) Quadratic Elongation: A Quantitative
466 Measure of Distortion in Coordination Polyhedra. Science, 172, 567–570.

467 Roelofsen, J.N. and Veblen, D.R. (1999) Relationships among zirconosilicates: examination by
468 cathodoluminescence and transmission electron microscopy. Mineralogy and Petrology, 67,
469 71-84.
470 Salvi, S. and Williams-Jones, A. E. (1995) Zirconosilicate phase relations in the Strange Lake
471 (Lac Brisson) pluton, Quebec-Labrador, Canada. American Mineralogist, 80, 1031-1040.
472 Sapozhnikov, A. N. and Kashaev, A.A. (1978) Features of the crystal structure of calcium-
473 containing elpidite. Kristallografiya (Soviet Physics - Crystallography), 23, 52-56.
474 Shannon, R.D. (1976) Revised effective ionic radii and systematic studies of interatomic
475 distances in halides and chalcogenides. Acta Crystallographica, A32, 751-767.
476 Sheldrick, G.M. (2003a) CELL_NOW, Program for unit cell determination. University of
477 Göttingen, Germany.
478 Sheldrick, G.M. (2003b) SADABS, Program for Empirical Absorption Correction of Area
479 Detector Data. University of Göttingen, Germany.
480 Sokolova, E., Hawthorne, F.C., Ball, N.A., Mitchell, R.H., and Della Ventura, G. (2006)
481 Vlasovite, $Na_2Zr(Si_4O_{11})$, from the Kipawa alkaline complex, Quebec, Canada: crystal-
482 structure refinement and infrared spectroscopy. Canadian Mineralogist, 44, 1349-1356.
483 Spek, A.L. (2009) Structure validation in chemical crystallography. Acta Crystallographica,
484 D65(2), 148-155.
485 Vladykin, N.V. (1983) Mineralogical-geochemical features of rare-metal granitoides of
486 Mongolia. Nauka. Novosibirsk, p.1-200. (in Russian).
487 Vladykin, N.V. (2013) Petrology and composition of Mesozoic rare-metal alkaline rocks in the
488 South Gobi Desert, Mongolia. Russian Geology and Geophysics, 54, 413-432.
489 Vladykin, N.V. and Kovalenko, V.I. (2006) Zirconium silicates. Armstrongite. In M.I.
490 Novgorodova, Ed., Minerals of Mongolia, p. 250-256, ЭКОСТ.

Vladykin, N.V., Kovalenko, V.I., Kashaev, A.N., Sapozhnikov, A.N., and Pisarskaya, V.A. (1973) A new mineral of calcium and zirconium, armstrongite. Doklady Akademii Nauk SSSR, 209, 1185-1188 (in Russian).

Vladykin, N.V., Kovalenko, V.I., and Dorfman, M.D. (1981) Mineralogical and geochemical pecularities of Khan Bogdo massif of an alkaline granites (MPR), p. 136. Moscow, Nauka. (in Russian).

Yakubovich, O.V., Karimova, O.V., Ivanova, A.G., Yapaskurt, V.O., Chukanov, N.V., and Kartashov, P.M. (2013) Ordering of cations in the voids of the anionic framework of the crystal structure of catapleiite. Crystallography Reports, 58(3), 401-411.

Yarmolyuk, V.V. and Kovalenko, V.I. (1991) Rift-oroginated magmatism of active continental margins and its ore potential, 263 p. Nauka, Moscow (in Russian).

Zubkova, N.V. and Pushcharovsky, D.Yu. (2008) New data on the crystal structures of natural zirconosilicates: structure refinements and ion-exchange behavior. Zeitschrift für Kristallographie, 223, 98-108.

Zubkova, N.V., Ksenofontov, D.A., Kabalov, Yu.K., Chukanov, N.V., Nedel'ko, V.V., Pekov, I.V., and Pushcharovsky, D.Yu. (2011) Dehydration-induced structural transformations of the microporous zirconosilicate elpidite. Inorganic Materials, 47(5), 506-512.

FIGURE CAPTIONS

FIGURE 1. Optical microscope picture of the armstrongite specimen and its host rock. Armstrongite-1 and Armstrongite-2 stand for armstrongite of the first and second generation, respectively.

FIGURE 2. Building blocks of the silicate layers of armstrongite. **(a)** Idealized wollastonite-like chain. **(b)** Idealized xonotlite-like chain. **(c)** Actual tetrahedral layer as derived from this study. **(d)** Silicate layer in armstrongite projected down to [010]. **(e)** Silicate layer in the studied armstrongite as seen down to [100]. **(f)** Armstrongite structure as seen along [001]. ZrO_6

517 octahedra, Ca-polyhedra, SiO_4 tetrahedra and oxygen atoms are drawn in green, pink, brown and
518 red, respectively.
519 **FIGURE 3.** FTIR spectrum obtained for the studied armstrongite. The region 1720-1520 cm^{-1} is
520 enlarged in the inset.
521 **FIGURE 4.** Perspective views of armstrongite projected down to [100], see Figure 4a, and
522 elpidite (space group P*bcm*) , see Figure 4b, from Cannillo et al. (1973) down to [010]. For
523 clarity, in the elpidite structure, the second Na atom in the octahedral plane has been omitted.
524 ZrO_6 octahedra, Ca-polyedra, Na-polyhedra, SiO_4 tetrahedra and oxygen atoms are drawn in
525 green, pink, yellow, brown and red, respectively.
526 **FIGURE 5.** The structure of elpidite from Cannillo et al. (1973) as seen along [100]. The dashed
527 blue square represents the subcell edges. ZrO_6 octahedra, Na atoms and SiO_4 tetrahedra and
528 oxygen atoms are drawn in green, yellow, brown and red, respectively.

Table 1. Average chemical composition (wt%) and atomic proportions (apfu) of the studied armstrongite compared with thosefrom literature

	Mongolian armstrongite			Canadian armstrongite		
	Arm_KB_2 (this work)	**Vladykin et al. (1973)** (Fe_2O_3 free analysis)	**Vladykin (1983);** Vladykin and Kovalenko (2006) (608/19a sample)	**Jambor et al. (1987)** (JEOL data)	**Jambor et al. (1987)** (CAMECA data)	**Salvi and Williams-Jones (1995)**
SiO_2	62.5(2)	60.76	59.16	61.2	60.4	63.4
Al_2O_3	0.02(1)	0.60	n.d.	n.d.	n.d.	n.d.
P_2O_5	n.d.	0.20	n.d.	n.d.	n.d.	n.d.
CaO	9.2(1)	9.25	7.47	9.2	9.4	10.0
Na_2O	0.03(1)	0.18	0.80	<0.1	<0.1	n.d.
MgO	b.d.l.	0.19	0.19	n.d.	n.d.	0.09
K_2O	0.01(1)	0.14	0.14	n.d.	n.d.	0.23
ZrO_2	20.9(2)	20.01	19.00	19.6	19.5	19.2
TiO_2	0.03(2)	0.12	0.11	n.d.	n.d.	0.16
Cr_2O_3	b.d.l.	n.d.	n.d.	n.d.	n.d.	n.d.
MnO	0.04(2)	n.d.	n.d.	n.d.	n.d.	n.d.
FeO	b.d.l.	n.d.	n.d.	n.d.	n.d.	0.07
Fe_2O_3	b.d.l.	n.d.	1.96	n.d.	n.d.	n.d.
ZnO	b.d.l.	n.d.	n.d.	n.d.	n.d.	n.d.
SrO	b.d.l.	n.d.	n.d.	n.d.	n.d.	n.d.
BaO	b.d.l.	n.d.	n.d.	n.d.	n.d.	n.d.
Nb_2O_5	n.d.	n.d.	0.34	n.d.	n.d.	0.35
La_2O_3	b.d.l.	0.015	0.17†	n.d.	n.d.	n.d.
Ce_2O_3	0.15(9)	0.05	0.33†	n.d.	n.d.	n.d.
Pr_2O_3	b.d.l.	0.05	0.07†	n.d.	n.d.	n.d.
Nd_2O_3	b.d.l.	0.02	0.28†	n.d.	n.d.	0.10
Sm_2O_3	b.d.l.	0.004	0.08†	n.d.	n.d.	n.d.
Eu_2O_3	0.1(1)	0.001	0.004†	n.d.	n.d.	n.d.
Gd_2O_3	b.d.l.	0.007	0.09†	n.d.	n.d.	n.d.
Dy_2O_3	b.d.l.	0.02	0.08†	n.d.	n.d.	n.d.
Ho_2O_3	b.d.l.	0.007	0.015†	n.d.	n.d.	n.d.
Er_2O_3	b.d.l.	0.04	0.092†	n.d.	n.d.	n.d.
Tm_2O_3	n.d.	0.02	0.02†	n.d.	n.d.	n.d.
Yb_2O_3	0.2(2)	0.05	0.07†	n.d.	n.d.	n.d.
Lu_2O_3	b.d.l.	0.01	0.006†	n.d.	n.d.	n.d.
Y_2O_3	n.d.	0.35	0.38	n.d.	n.d.	n.d.
REE+Y_2O_3		0.64	1.68	n.d.	n.d.	n.d.
H_2O	6.2*	8.0**	8.84	10.0***	10.7***	n.d.
Total	99.38	100.09	99.70	100	100	93.50
Si	6.00	5.92	n.r.	6.06	6.04	n.r.
Al		0.07	n.r.			n.r.
P		0.02	n.r.			n.r.
Ca	0.96	0.96	n.r.	0.98	1.01	n.r.
Na		0.03	n.r.			n.r.
Mg		0.02	n.r.			n.r.
K		0.01	n.r.			n.r.
Zr	0.99	0.96	n.r.	0.95	0.95	n.r.
Ti		0.01	n.r.			n.r.
Ce	0.01		n.r.			n.r.
Yb	0.01		n.r.			n.r.
REE		0.03	n.r.			n.r.
H_2O	2.02	2.58	n.r.	3.31	3.57	n.r.

Notes: b.d.l. = below detection limit; n.d. = not determined;n.r. = not reported;†calculated from the data in Table 150 of Vladykin and Kovalenko (2006); *H_2O as derived from structural refinement data (see text for detail); **H_2O from density measurements; ***H_2O obtained by difference from 100 wt%.

Table 2. Selected crystallographic data for the studied armstrongite

	Mongolian armstrongite			Canadian armstrongite
	Arm_KB_2	**Vladykin et al. (1973)**	**Kabalov et al. (2000)**	**Jambor et al. (1987)**
Crystal size (mm^3)	0.26x0.10x0.10			
Space group	*C*2/*m*	*C*2, *Cm*, *C*2/*m*	*C*2	*I*2/*m*, *I*2, *Im*
***a* (Å)**	14.0178(7)	14.04	14.018(1)	13.599(9)
***b* (Å)**	14.1289(6)	14.16	14.133(1)	14.114(9)
***c* (Å)**	7.8366(3)	7.81	7.840(1)	7.833(4)
β (°)	109.436(3)	109.55	109.40(1)	103.41(5)
Cell volume ($Å^3$)	1463.6(1)	1463.2	1465.0	1462.4
μ (mm^{-1})	1.69			
Measured reflections	18041			
Independent reflections	9762			
$R_{merging}$ [$R_{(int)}$] (%)	4.5			
h_{min}, h_{max}	-23, 22			
k_{min}, k_{max}	-23, 23			
l_{min}, l_{max}	-13, 13			
Reflections used ($I > 3\sigma(I)$)	5708			
No. of refined parameters	126			
Goof[a]	1.077			
***R*[b] [on *F*] (%)**	3.32			
R_w[c] [on F^2] (%)	2.92			
$\Delta\rho_{min}/\Delta\rho_{max}$ ($e^-/Å^3$)	-2.78/2.58			
Twin element ratio	0.6176(5) : 0.3824(5)			

Table 3. Atomic coordinates, equivalent isotropic (Å^2) and anisotropic displacement parameters of the studied armstrongite

Site	Atom type	*x/a*	*y/b*	*z/c*	*U*(iso)	U_{11}	U_{22}	U_{33}	U_{12}	U_{13}	U_{23}
Zr1	**Zr^{4+}**	0.25	0.25	0	0.0102	0.01089(6)	0.00812(5)	0.01256(6)	-0.00063(6)	0.00502(5)	-0.00104(6)
Ca1	**Ca^{2+}**	0.25436(4)	0.5	0.04824(6)	0.0200	0.0296(2)	0.0108(1)	0.0251(2)	0	0.0163(2)	0
Si1	**Si**	0.18699(3)	0.61399(3)	0.33903(5)	0.0128	0.0145(1)	0.0099(1)	0.0148(1)	0.0014(1)	0.0061(1)	0.0020(1)
Si2	**Si**	0.34112(3)	0.61018(2)	0.73110(5)	0.0122	0.0153(1)	0.0081(1)	0.0148(1)	-0.0006(1)	0.0072(1)	-0.0011(1)
Si3	**Si**	0.00363(3)	0.74257(3)	0.30239(5)	0.0129	0.0115(1)	0.0114(1)	0.0164(1)	0.0006(1)	0.0055(1)	0.0001(1)
O1	**O**	0	0.7679(1)	0.5	0.0287	0.0368(9)	0.035(1)	0.0189(6)	0	0.0150(6)	0
O2	**O**	0.2598(1)	0.63983(9)	0.5392(1)	0.0237	0.0310(6)	0.0219(5)	0.0153(5)	-0.0004(4)	0.0037(4)	0.0011(4)
O3	**O**	0.29672(8)	0.62811(7)	0.8916(1)	0.0166	0.0207(4)	0.0136(4)	0.0185(4)	-0.0002(3)	0.0105(4)	0.0006(3)
O4	**O**	0.22858(9)	0.65291(8)	0.1858(1)	0.0183	0.0255(5)	0.0147(4)	0.0181(4)	0.0027(3)	0.0116(4)	0.0004(4)
O5	**O**	0.1824(1)	0.5	0.3095(2)	0.0206	0.0232(7)	0.0106(5)	0.0299(8)	0	0.0113(6)	0
O6	**O**	0.3703(1)	0.5	0.7273(2)	0.0216	0.0298 (8)	0.0093(5)	0.0310(8)	0	0.0170(6)	0
O7	**O**	0.44478(9)	0.66733(8)	0.7598(2)	0.0220	0.0219(5)	0.0177(4)	0.0278(5)	0.0012(4)	0.0103(4)	-0.0077(4)
O8	**O**	0.07373(9)	0.64942(9)	0.3147(2)	0.0250	0.0201(5)	0.0189(5)	0.0380(6)	0.0042(4)	0.0123(4)	0.0076(4)
O9	**O**	-0.10488(8)	0.72320(9)	0.1627(2)	0.0224	0.0139(4)	0.0229(5)	0.0264(5)	-0.0001(4)	0.0012(4)	-0.00021(3)
O_w10	**O**	0.0883(2)	0.5	-0.1431(5)	0.0641	0.042(1)	0.035(1)	0.091(2)	0	-0.010(1)	0
O_w11	**O**	0.4154(2)	0.5	0.2651(5)	0.0577	0.024(1)	0.041(1)	0.099(2)	0	0.009(1)	0
H101	**H**	0.0461	0.5489	-0.1675	0.0951						
H111	**H**	0.4565	0.4508	0.2833	0.0836						

Table 4. Bond lengths (Å) and polyhedral volumes (Å^3) for the studied armstrongite compared to those refined in *C*2 s.g. from Kabalov et al. (2000). X-ray and EPMA mean atomic numbers (electrons, e$^-$) and mean interatomic distances as derived by cation distribution for the studied sample are also reported, together with the lengths (Å) and angles (°) of H-bonds.

	Arm_KB_2		Kabalov et al. (2000)		
		Tetrahedra			
Si1-O4$_{ush}$	1.597(1)	**Si1-O5$_{ush}$**	1.52(5)	**Si2-O7$_{ush}$**	1.60(6)
Si1-O5$_{sh}$	1.6253(4)	**Si1-O3$_{sh}$**	1.59(5)	**Si2-O4$_{sh}$**	1.60(6)
Si1-O2$_{sh}$	1.603(1)	**Si1-O9$_{sh}$**	1.59(9)	**Si2-O9$_{sh}$**	1.69(9)
Si1-O8$_{sh}$	1.614(1)	**Si1-O11$_{sh}$**	1.62(5)	**Si2-O13$_{sh}$**	1.60(6)
<Si1-O>	1.610(2)	**<Si1-O>**	1.58	**<Si2-O>**	1.62
Volume	2.132	**Volume**	1.889	**Volume**	2.147
Si2-O3$_{ush}$	1.598(1)	**Si3-O6$_{ush}$**	1.59(4)	**Si4-O8$_{ush}$**	1.59(4)
Si2-O6$_{sh}$	1.6124(6)	**Si3-O4$_{sh}$**	1.62(4)	**Si4-O3$_{sh}$**	1.59(5)
Si2-O2$_{sh}$	1.611(1)	**Si3-O10$_{sh}$**	1.64(8)	**Si4-O10$_{sh}$**	1.63(7)
Si2-O7$_{sh}$	1.611(1)	**Si3-O12$_{sh}$**	1.67(5)	**Si4-O14$_{sh}$**	1.62(7)
<Si2-O>	1.608(2)	**<Si3-O>**	1.63	**<Si4-O>**	1.61
Volume	2.131	**Volume**	2.212	**Volume**	2.106
Si3-O9$_{ush}$	1.575(1)	**Si5-O16$_{ush}$**	1.57(5)	**Si6-O15$_{ush}$**	1.62(4)
Si3-O1$_{sh}$	1.6067(6)	**Si5-O1$_{sh}$**	1.60(5)	**Si6-O2$_{sh}$**	1.64(4)
Si3-O7$_{sh}$	1.617(1)	**Si5-O11$_{sh}$**	1.66(7)	**Si6-O13$_{sh}$**	1.65(6)
Si3-O8$_{sh}$	1.626(1)	**Si5-O12$_{sh}$**	1.62(7)	**Si6-O14$_{sh}$**	1.63(7)
<Si3-O>	1.606(2)	**<Si5-O>**	1.61	**<Si6-O>**	1.64
Volume	2.123	**Volume**	2.134	**Volume**	2.200
e$^-$$_{X\text{-}ref}$	84.00				
e$^-$$_{EPMA}$	84.00				
<Si-O>$_{X\text{-}ref}$	1.608				
<Si-O>$_{EPMA}$	1.610				
		Zr-octahedra			
Zr-O4 (x2)	2.093(1)	**Zr-O5**	2.23(5)		
Zr-O3 (x2)	2.118(1)	**Zr-O6**	2.15(4)		
Zr-O9 (x2)	2.045(1)	**Zr-O7**	2.01(5)		
<Zr-O>	2.086(2)	**Zr-O8**	2.07(5)		
Volume	11.983	**Zr-O15**	2.11(3)		
		Zr-O16	2.02(3)		
		<Zr-O>	2.10		
		Volume	11.943		
e$^-$$_{X\text{-}ref}$	40.00				
e$^-$$_{EPMA}$	39.60				
<Zr-O>$_{X\text{-}ref}$	2.085				
<Zr-O>$_{EPMA}$	2.070				
		Ca-polyhedra			
Ca-O3 (x2)	2.371(1)	**Ca-O5**	2.51(5)		
Ca-O4 (x2)	2.494(1)	**Ca-O6**	2.30(5)		
Ca-O5	2.566(2)	**Ca-O7**	2.64(5)		
Ca-O$_w$10	2.312(3)	**Ca-O8**	2.55(5)		
Ca-O$_w$11	2.330(3)	**Ca-O9**	2.69(3)		
<Ca -O>	2.420(5)	**Ca-O17**	2.43(3)		
Volume	21.557	**Ca-O18**	2.40(3)		
		<Ca-O>	2.50		
e$^-$$_{X\text{-}ref}$	20.00	**Volume**	22.980		
e$^-$$_{EPMA}$	20.48				
<Ca-O>$_{X\text{-}ref}$	2.420				
<Ca-O>$_{EPMA}$	2.388				
		H-bonds			
O$_w$10-H101	0.89	**H101···O8**	2.21	**O$_w$10-O8**	3.06
O$_w$11-H111	0.88	**H111···O7**	2.26	**O$_w$11-O7**	3.12
O$_w$10-H101···O8	161.6				
O$_w$11-H111···O7	162.6				

Note: sh= shared;ush =unshared.

Table 5. Selected distortion parameters for the studied armstrongite compared to those from Kabalov et al. (2000)

	Arm_KB_2			Kabalov et al. (2000)					
				Tetrahedra					
	Si1	**Si2**	**Si3**	**Si1**	**Si2**	**Si3**	**Si4**	**Si5**	**Si6**
BLD	0.615	0.311	0.986	1.889	1.593	1.320	1.392	1.661	0.519
ELD	1.424	0.855	0.812	4.402	3.825	1.999	3.232	1.308	2.701
TAV	11.958	5.494	4.071	54.373	43.852	19.550	48.444	6.881	38.233
TQE	1.003	1.001	1.001	1.015	1.013	1.005	1.012	1.002	1.010
$\Delta z_{[100]}$		0.171				0.584			
$\Delta z_{[010]}$		0.572				0.828			
				Zr-octahedra					
BLD		1.302				3.144			
ELD		2.920				7.036			
OAV		18.769				68.511			
OQE		1.006				1.022			
				Ca-polyhedra					
BLD		3.48				4.274			
ELD		14.456				33.878			

Notes: BLD: bond-length distortions (Renner and Lehmann 1986); ELD: edge-length distortion (Renner and Lehmann 1986); TAV: tetrahedral angle variance (Robinson et al. 1971);TQE: tetrahedral quadratic elongation (Robinson et al. 1971); $\Delta z = (z^{Oush}_{max}-z^{Oush}_{min})$: departure from complanarity of the unshared O atomsalong [100] and [010]; OAV: octahedral angle variance (Robinson et al. 1971); OQE: octahedral quadratic elongation (Robinson et al. 1971).
Errors on distortion parameters, estimated by varying the refined positional parameters within one standard deviation, are in the following ranges: ≤ 10% for angles, ≤ 8% bond/edge lengths distortions, ≤ 1% for sheet corrugations.

Table 6. Band position (cm^{-1}), assignment for the hydrogen absorption bands of the studied and literature selected zircon-silicate belonging to the zircon-zeolite family

Specimen	Occurrence	Chemical formula	Band position	Band assignment	References
Armstrongite	Khan Bogdo (Mongolia)	$(Ca_{0.96}Ce_{0.01}Yb_{0.01})$ $Zr_{0.99}Si_{6.00}O_{15}\cdot 2.02H_2O$	3700-3300 1638, 1610	H_2O Stretching H_2O Bending	This study
Elpidite	Khan Bogdo (Mongolia)	$(Na_{1.65}Ca_{0.15}K_{0.01}H_{0.03})$ $ZrSi_6O_{15}\cdot 3H_2O$	3551, 3505, 3453 1647, 1638	H_2O Stretching H_2O Bending	Grigor'eva et al. (2011)
Elpidite	Mount Alluaiv (Kola Peninsula, Russia)	$(Na_{1.98}K_{0.01})(Zr_{1.02}Nb_{0.03}Hf_{0.01})$ $(Si_{5.92}Al_{0.02})O_{15}\cdot 3.28H_2O$	3540, 3490, 3435 1660, 1640, 1620	H_2O Stretching H_2O Bending	Zubkova et al. (2011)
Catapleiite	Zhil'naya Valley (Kola Peninsula, Russia)	$(Na_{1.5}Ca_{0.2})[ZrSi_3(O,OH)_9]\cdot 2(H_2O,F)$	3575, 3502 3280, 3080 1660, 1646	H_2O Stretching Acidic OH^- groups H_2O Bending	Yakubovich et al. (2013)
Lemoynite	St. Hilaire (Québec)	$(Na,Ca)_3Zr_2Si_8O_{22}\cdot 8H_2O$	3600, 3400 1668, 1615	OH^- region H_2O Bending	Perrault et al. (1969)
Eudialyte	St.-Hilaire: (Québec) Andrup Fjord (Greenland)	$Na_{15}Zr_3Si_{25}O_{73}(O, OH, H_2O)_3$	3440, 3150 1655	OH^- Stretching H_2O Bending	Johnsen and Grice (1999)
Monteregianite	St. Hilaire (Québec)	$(Na_{4.66}K_{1.80})(Y_{1.68}Ca_{0.18}Mg_{0.06}Ba_{0.04})$ $(Si_{15.87}Al_{0.16})O_{38}\cdot 10H_2O$	3610, 3510, 3460	H_2O Stretching	Chao (1978)

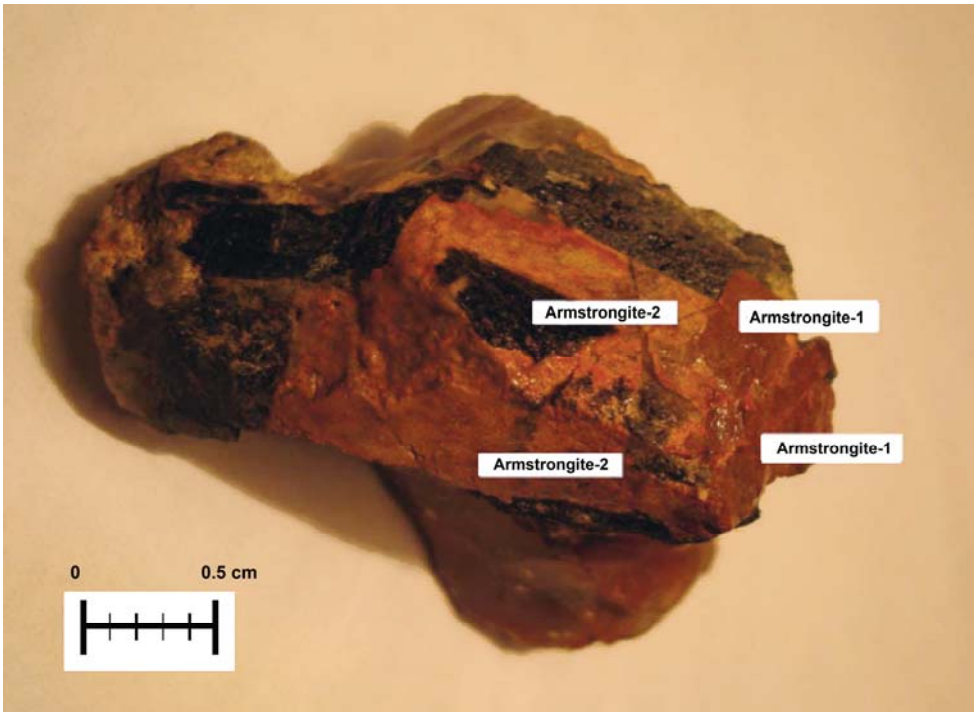
Armstrongite-2
Armstrongite-1
Armstrongite-2
Armstrongite-1
0
0.5 cm

Figure 1

Figure 2a

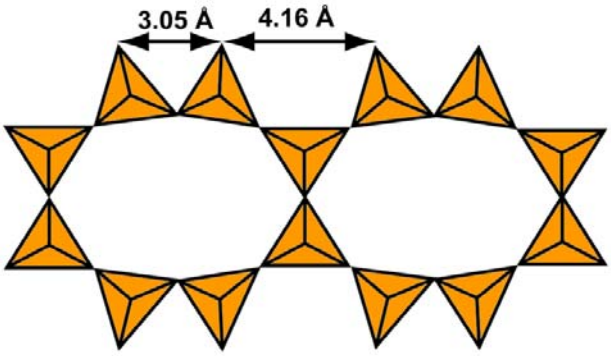

Figure 2b

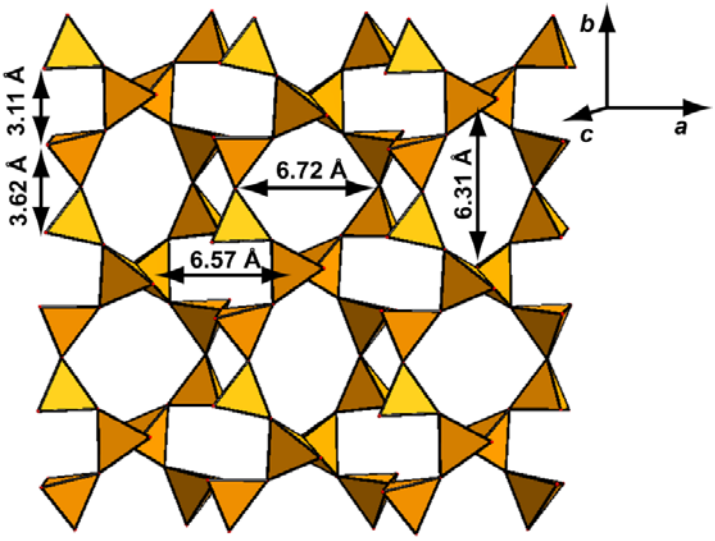

Figure 2c

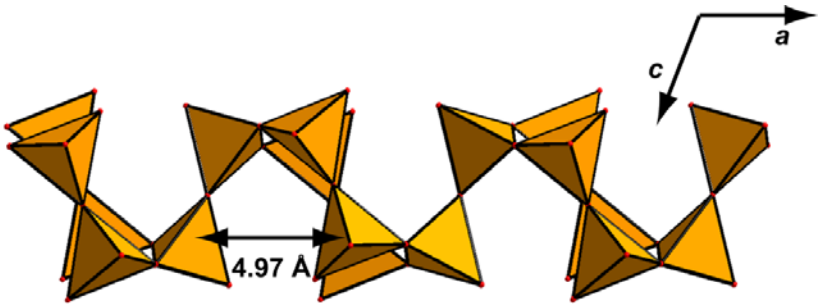

Figure 2d

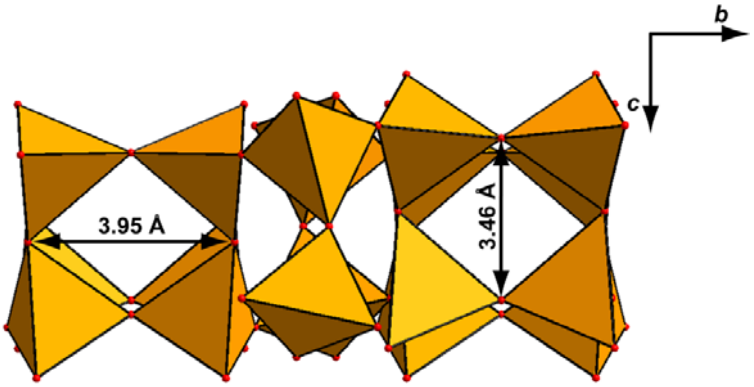

Figure 2e

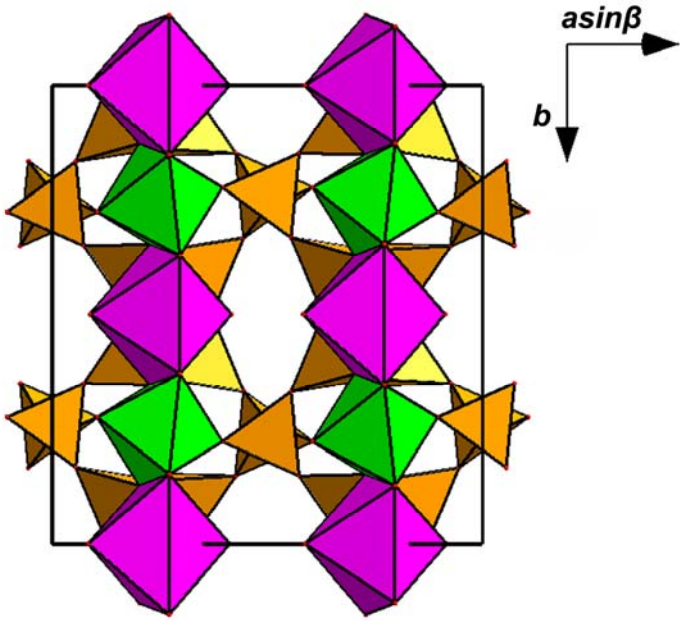

Figure 2f

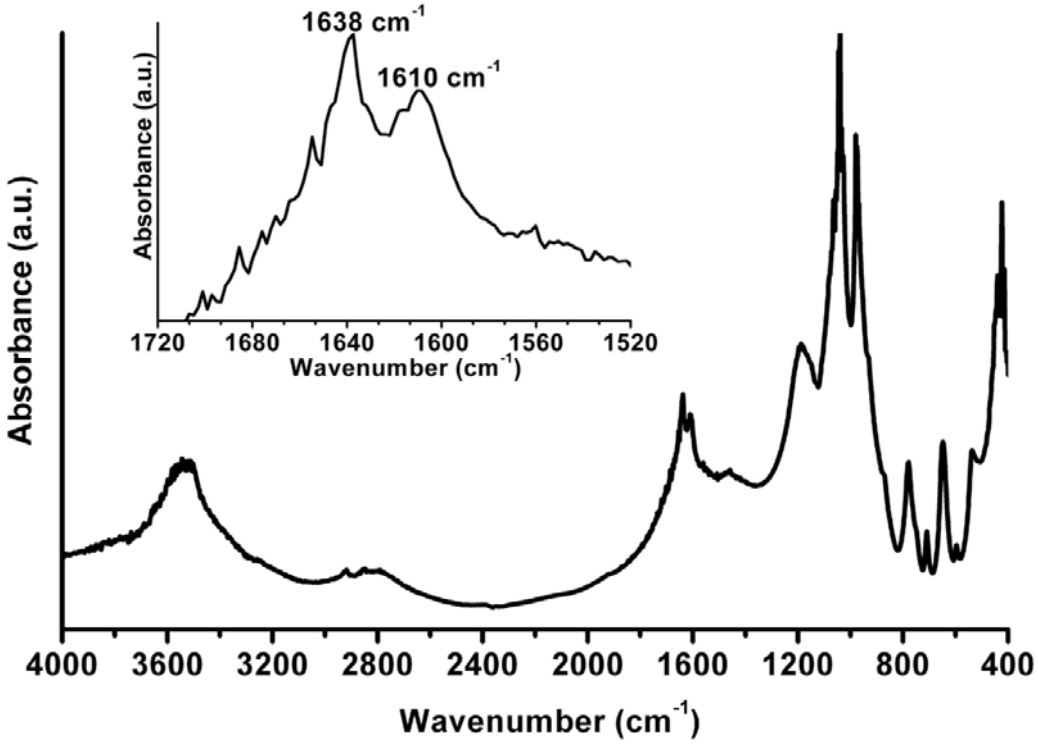
1638 cm-1
1610 cm-1
Absorbance (a.u.)
1720
1680
1640
1600
1560
1520
Wavenumber (cm-1)
Absorbance (a.u.)
4000
3600
3200
2800
2400
2000
1600
1200
800
400
Wavenumber (cm-1)

Figure 3

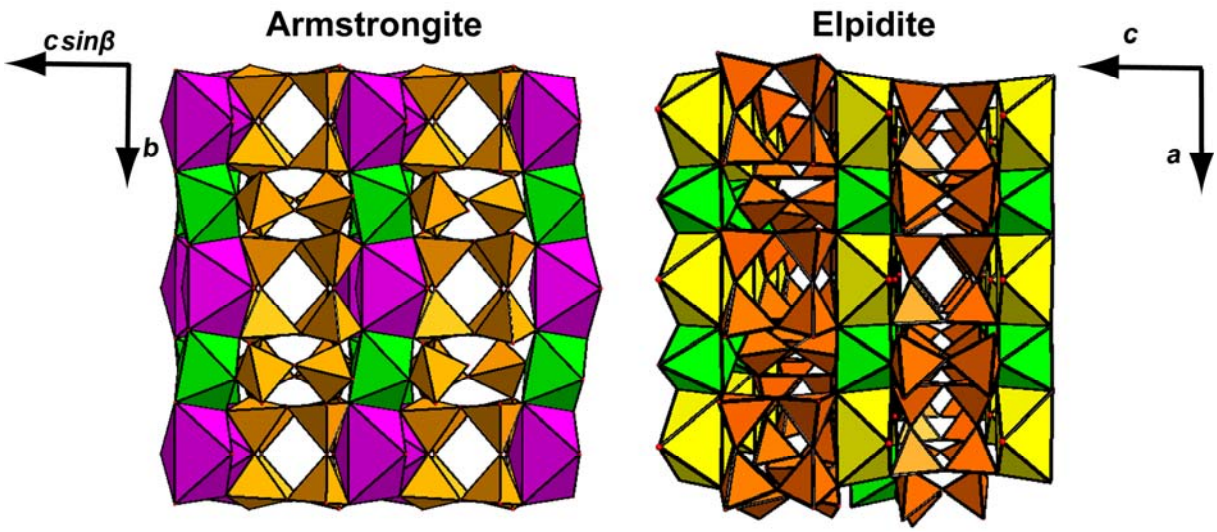

a) **b)**

Figure 4

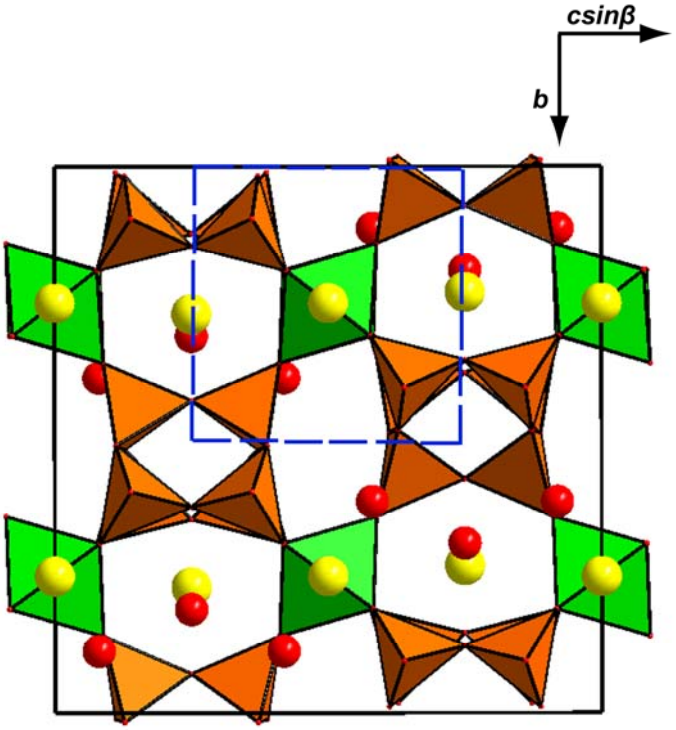

Figure 5